COMMAT 1166
27 February 2002 Disk used

ARTICLE IN PRESS

No. of Pages 9, DTD = 4.3.1
SPS-N, Chennai

ELSEVIER

Computational Materials Science xxx (2002) xxx–xxx

COMPUTATIONAL MATERIALS SCIENCE

www.elsevier.com/locate/commatsci

Atomic processes at bonded Si-interfaces studied by molecular dynamics: tayloring densities and bandgaps?

Kurt Scheerschmidt *, Detlef Conrad [1], Alexander Belov [2]

Max Planck Institute of Microstructure Physics, Weinberg 2, D-06120 Halle/Saale, Germany

Received 20 November 2001

Abstract

Molecular dynamics simulations using empirical potentials have been employed to describe atomic interactions at interfaces created by the macroscopic wafer bonding process. Investigating perfect or distorted surfaces of different semiconductor materials enables one to study the elementary processes and the resulting defects at the interfaces, and to characterize the ability of the potentials used. Twist rotation due to misalignment and bonding over steps influence strongly the bondability of larger areas and create new types of structural units at the bonded interfaces. Ab initio density functional based simulations establish the structural units to be the stable minimum configurations and enable to predict modified electronic properties. © 2002 Published by Elsevier Science B.V.

Keywords: Molecular dynamics; Wafer bonding; Bonded interfaces; Structural units; Ab initio density functional theory; Band structure; Twist boundary; Dreidl

1. Introduction

Wafer bonding, i.e. the creation of interfaces by joining two wafer surfaces, has become an attractive method for many practical applications in microelectronics, micromechanics or optoelectronics [1,2]. The macroscopic properties of bonded materials are mainly determined by the atomic processes at the interfaces during the transition from the adhesion state to the chemical bonding. Thus, the description of the atomic processes is of increasing interest to support the experimental investigations or to predict the bonding behaviour. While, in principle, it is now possible to predict material properties by using quantum-theoretical ab initio calculations with a minimum of free parameters, the only method to simulate atomic processes with macroscopic relevance is the molecular dynamics (MD) method using suitably fitted many-body empirical potentials. Such simulations enable a sufficiently large number of particles and relaxation times up to μs to be considered. However, the electronic structure and the nature of the covalent bonds can only be described

* Corresponding author. Tel.: +49-345-558-2910; fax: +49-345-558-2917.

E-mail address: schee@mpi-halle.de (K. Scheerschmidt).. *URL:* http://www.mpi-halle.de.

[1] Present address: Avant! Corporation, Radeberger Str., 01099 Dresden, Germany.

[2] Present address: Institut für Ionenstrahlphysik und Materialforschung, Forschungszentrum Rossendorf, Germany.

0927-0256/02/$ - see front matter © 2002 Published by Elsevier Science B.V.
PII: S0927-0256(02)00162-3

UNCORRECTED PROOF

indirectly. Therefore, small relevant structural units must be investigated directly using ab initio calculations based on the density functional theory (DFT) to enhance the understanding in detail and to support the fit of the empirical potentials. In addition, it is of importance to find physically motivated semiempirical potentials starting mostly with the moments of the electron density and using tight-binding (TB) representations [3–5].

The MD simulations have successfully been used to describe ultra-high-vacuum bonding experiments for Si(1 0 0) [6], hydrogen passivated hydrophobic bonding processes [7], and to analyze the defect structure at bonded interfaces [8–10]. Simulations for SiC [11] were possible using the Tersoff [12,13] potential. It is well suited also to describe the SiC(0 0 0 1)-3×3 and $\sqrt{3} \times \sqrt{3}$R30° surface reconstructions [11]. A comparison with TB and DFT results shows that even the bond length and energy differences of the different reconstructions are correctly revealed. The prediction of the bondability of diamond has been performed using a TB based empirical bond-order potential (BOP [14]). The TB level is necessary to describe correctly the π-bonds. Both the TB-MD and the semiempirical method using BOP show the same bonding behaviour, however, the BOP enables one to use far more atoms in the calculation. Different techniques of electron microscopy structure imaging have been applied to investigate the bonded interfaces and resulting defects at an atomic level [15], the MD relaxed structures are the basis to compare simulated and experimental images, which in combination with calculated IR-spectra provide a good experimental evidence.

The analysis of the structural details of various relaxed interacting Si(0 0 1) surfaces [8–10], in particular for 90° twist rotation [8], have shown that special structural units may occur [9]. DFT calculations revealed the stability and relative energy minima of these units. However, in both the empirical MD and the DFT simulations the so called "dreidl" configuration is the lowest energy configuration. A similar structural unit was first proposed by Mostoller et al. [16] as the core structure of dislocation intersections. In the present paper the band structures of the dreidl and a second structural unit are discussed. In addition, new crystalline structures for Si by repeating of the dreidl structure in three dimensions are investigated by DFT simulations. Different structures can be obtained by a different stacking sequence of the dreidls. Here, the results are presented concerning the two structures with the smallest unit cells having 12 and 24 atoms, respectively, and a relation to low density phases is established.

2. Empirical molecular dynamics

The method of MD solves Newton's equations of motion for a system of particles yielding all their trajectories. The calculations are performed with a fifth-order predictor–corrector algorithm using constant volume (NVE ensemble) or constant pressure (NpT ensemble) and time steps of the order of 0.25 fs to ensure the proper calculation of surface modes. NVE is preferred for free surfaces and simulations to calculate diffusion processes, whereas NpT enables the relaxation of the cell dimensions and the application of an outer pressure. To describe an energy flux or dissipation into a macroscopic embedding substrate periodic boundary conditions are applied solely parallel to the interfaces. The system temperature is therefore controlled per time step by slightly rescaling the velocities of the atoms in the outer layers of the structure models only. In addition, for straight defects created at the interfaces the system is coupled elastically to the bulk. Simple force-field potentials are restricted in their validity to small deviations from the equilibrium. A better potential most often used for semiconductors is the Stillinger–Weber (SW) potential, having additionally three-body interactions [17]. It allows the next neighbour interaction to be included by rescaling, which is a presupposition to the simulation of the dynamical behaviour without preordered surfaces and prescribed topology. The potential of Tersoff [12,13] with different parametrizations TI–TIII has the shape of a bond order, which is a completely different functionality. The bonds are weighted by the bond order including all many body interactions over neighbours different from the actual bonding pair. It predicts the asymmetric reconstruction with four-fold coordinated atoms at Si

interfaces with defects. Therefore it was applied to investigate the cores of different defects left after bonding two wafers. Parametrizations exist also to describe the silicon–hydrogen interaction, hydrocarbons, SiC, Ge, etc. (cf., e.g., [18]), thus hydrogenated Si(0 0 1) surfaces [7] and Si–SiC interactions [11] are investigated, too. Because of the short range of the Tersoff potential it was supposed that the bond topology is given by the usual process starting with separated Si blocks of a suitable surface structure and orientation (surface reconstruction, steps) and applying long-range potentials initially. Compared to each other [19], the empirical potentials offer advantages and disadvantages in range of validity, physical meaning, fitting and accuracy as well as applicability. Such restrictions exist for other potential types, too, e.g., the (modified) embedded atom approximation (MEAM, [20]), and no potential is applicable for long range interactions. In addition, the interatomic forces in covalent solids can only be completely described if the influence of the local environment according to the electronic structure is included. TB approximations allow to develop physically motivated potentials, starting from analysis of the band energy. The repulsive energy is assumed to be an embedded pair interaction, the promotion energy reflects the energy difference of valence s and p electrons. The band energy is the expansion of the electronic energy into hopping matrix elements and bond order terms. A second moment approximation (BOP2) of the TB model can be used to establish a general form at the level of the Tersoff potential with at least only four free fit parameters [4]. A further enhancement is based on BOP4 [5], which is given up to the fourth-level continued fraction of the Greens function. Its ability is demonstrated in the application to diamond wafer bonding [14].

3. Ab initio simulations

The ab initio simulations were carried out using the code CASTEP; the details are given elsewhere [21]. Here the calculations were performed using the pseudopotential method within the local density approximation (LDA) for the optimization of the cell geometry and the atomic positions. The ions are described by ultra-soft pseudopotentials [22]. The wave functions are expanded using a plane wave basis with an energy cut-off of 120 eV. Special **k**-points according to the scheme of Monckhorst and Pack [23] were used to sample the Brillouin zone, chosing $2 \times 2 \times 2$ sets this yields 2 symmetrized points. In order to allow the comparison of the total energies, a **k**-point spacing is applied which is similar for all the structures considered. With the energy cut-off and **k**-points chosen it is possible to reproduce the experimental lattice constant of Si with an accuracy of better than 2%. A similar test with the four-fold-coordinated clathrates Si(3 4) and Si(4 6) [24], built by mixing dodecahedra with 16-hedra or icosahedra in a cubic lattice, yields to differences in the total energy per atom of 0.22 and 0.17 eV, respectively, whereas the volume ratio to the diamond structure of 1.17 is exact reproduced. Calculations for various other structures were carried out for comparison, too, the details will be published in a forthcoming paper elsewhere together with enhanced energy investigations of the dreidl arrangements discussed below.

4. The structure of bonded interfaces

A MD simulation which starts with two perfect and parallel-oriented Si blocks, perfectly aligned 2×1 reconstructed (1 0 0) surfaces, and applying a slow heat transfer approach, yields to perfectly bonded structures [6,7]. However, a fast heat transfer, a starting configuration, with the dimer rows in orthogonal domain orientation, or including steps or small rotational misorientations, result in configurations no longer perfectly coordinated. The energy flux at surfaces is the driving force for the bonding process. The upper terraces behave like perfect surfaces, i.e., a weak attraction owing to the next neighbour interaction initiates the dimers to rearrange and to create new bonds. The energy the bonds have gained dissipates, increasing the kinetic and elastic energies of the bulk. The resulting avalanche effect implies the bonding of the lower terraces, too. After bonding over double layer steps, a disturbed interface and

UNCORRECTED PROOF

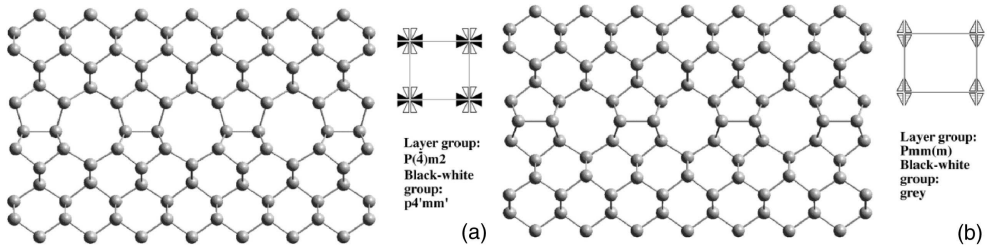

Fig. 1. Structural models of the two 90° twist boundaries with lowest energy: (a) $\bar{4}2m$-dreidl configuration, (b) Pmm(m) configuration with coordination defects (for details see text and [8]).

defects are left which may finally relax to 60° glide- or shuffle-set dislocations accompanied by a row of vacancies [8–10]. Monolayer steps rotate the dimerization direction in the neighbouring domains and give rise to a stacking fault. The interfaces between, or outside, the single-layer steps are characterized by a 90° twist-rotation: Fig. 1 shows the two configurations with the lowest energy found in empirical MD simulations [8].

The 90° twist boundary and using the SW potential yields to a metastable five-fold coordinated interface with a symmetric structure normal to the interface characterized by a Pmm(m) layer group (Fig. 1b). Using the Tersoff or BOP-like potentials and metastable or well-prepared starting configurations yields to further structure relaxation and energy minimization. Fig. 1a shows the relaxed configuration through the Tersoff potential, which is (2×2) reconstructed and can be imaged to consist of structural units with a $\bar{4}2m$ (D_{2d}) point group symmetry, called the $\bar{4}2m$-dreidl (cf. Fig. 2a) in analogy to the mm2-dreidl in [16]. The $\bar{4}2m$-dreidl fits two rotated half crystals of minimal structural disorder and four-fold coordination described by a P($\bar{4}$)m2 layer symmetry. The interface energy is reduced by approximately 20%. The detailed structural and energetical characterization of the different structural units found by empirical MD are discussed in [8].

Here it is of interest that the dreidl structure is found to be the minimum energy configuration in DFT-LDA simulations, too. However, the energies differ from those given in [8], one yields 0.45 and 1.39 J/m^2 for the P($\bar{4}$)m2 and the Pmmm configurations, which is 50% less or 20% higher than the corresponding TIII values, respectively.

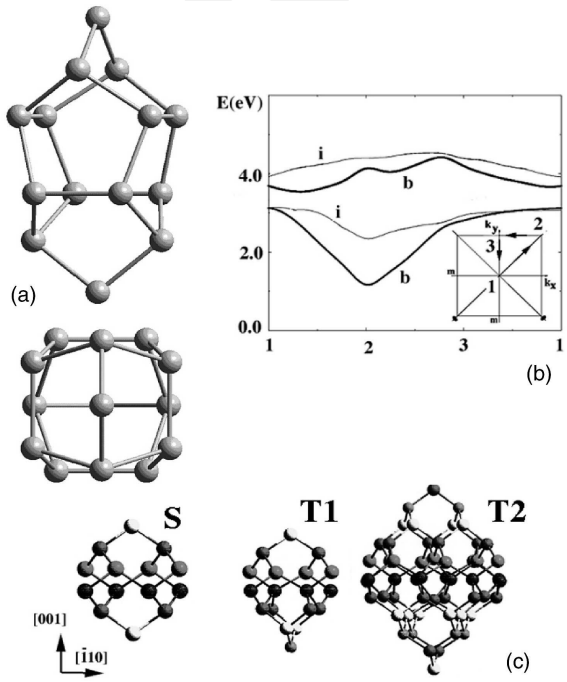

Fig. 2. Defect core reconstructions: (a) $\bar{4}2m$-dreidl as the structural unit of a 90° twist boundary, (b) DFT-LDA band structure of the dreidl interface (bands i) versus a bulk silicon crystal (bands b), and (c) core structures of the screw misfit dislocations (S) of bonded interfaces with small twist rotations and the two stable nodes for fully TIII-relaxed screw network intersections (T1,T2).

Fig. 2b shows the band structure compared to perfect bulk Si. In Fig. 3 the electron density maps of both the structural units of the bonded interfaces from Fig. 1 are given, the details of the band structure calculations are discussed in the next section. Applying a small twist angle as a rota-

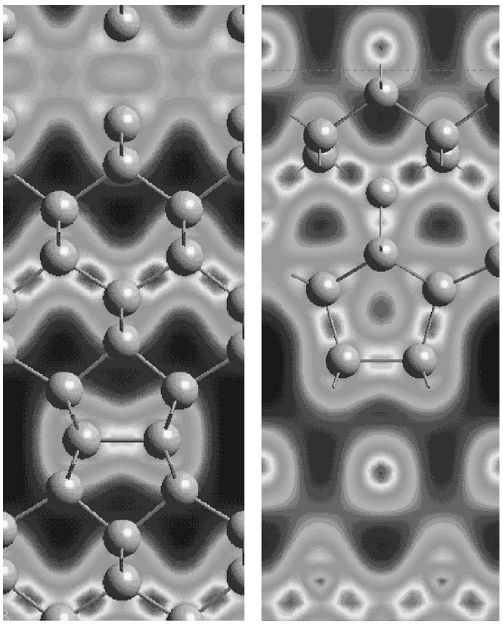

Fig. 3. Electron density maps of the structural units of bonded interfaces: (a) Pmmm and (b) P($\bar{4}$)m2 ($\bar{4}2m$-dreidl) symmetry.

tional misorientation results in a mosaic-like bonded interface structure [6]. After bonding and sufficient relaxation under slow heat transfer conditions, almost all atoms have a bulk-like environment separated by misfit screw dislocations, which may have a high rate of kinks and form a network. Similarly, a prescribed network of two sets of a/2[1 1 0] screw dislocations, which accommodate a small rotationally twist, is relaxing into a configuration by breaking symmetry [9]: It has twice the period of the array distance related to the twist angle and shows two different types of intersections (cf. Fig. 2c: T1, T2). They are formed by symmetrical characteristic groups of atoms having the same point group symmetry 222 (D_2) as the core structures of individual screws (S). Most of the atoms forming T1 remain four-fold with large bond-angle and bond-length distortions, but there are two atoms in the unit with a five-fold surrounding. The T2-nodes are formed by more complicated atomic groups, however, showing solely a four-fold coordination. MD simulations as well as TEM and HREM investigations showed further [10] that the screw dislocations forming the network of the (0 0 1) low-angle twist grain boundary can dissociate intrinsically into two 30° partials along the {1 1 1} glide plane.

Independently from the chosen twist angles and box dimensions the investigated structures yield finally bond energies of approximately 4.5 eV/atom at 0 K [25]. The energy gain, however, is directly related to the twist angle, a maximum of approximately 0.05 eV was found near 6°, within the investigated range from 2.8° to 12.7°. The values are slightly modified if additional steps or holes are included at the surfaces before bonding simulation starts. The maximum energy gain is related to a change of the bonding behaviour itself: Whereas all simulations with parallel dimerization at start clearly demonstrate the creation of screw dislocation networks, for orthogonal dimerization or small twist angles this is no longer valid. The higher the annealing temperature, the better the screw network formation.

5. The dreidl band structure

Figs. 4 and 5 present the DFT-LDA band structure calculations for both interfaces discussed in the previous section. The structural units of the Pmmm and the P($\bar{4}$)m2 interfaces are arranged within relatively small supercells for the periodic continuation enabling the applicability of the code CASTEP on workstations. The structures chosen for the ab initio simulation are shown as 2×2 representation of the supercells in Figs. 4a and 5a for the [1 1 0] projection and Figs. 4b and 5b for the [1 $\bar{1}$ 0] projection. One reveals that the supercell in Fig. 4 contains two Pmmm structural units, whereas each supercell of Fig. 5 has only one $\bar{4}2m$-dreidl, thus the corresponding interface distances are approximately 1.1 and 1.8 nm, respectively, which may influence the results.

The DFT-LDA band structures of the Pmmm structural unit and the $\bar{4}2m$-dreidl are shown in Figs. 4c and 5c, respectively. The band structure overview and the enlarged band gap region are presented for both interfaces, the Fermi energy is indicated in the band gap. Whereas the $\bar{4}2m$-dreidl has an indirect band gap of approximately 0.9 eV

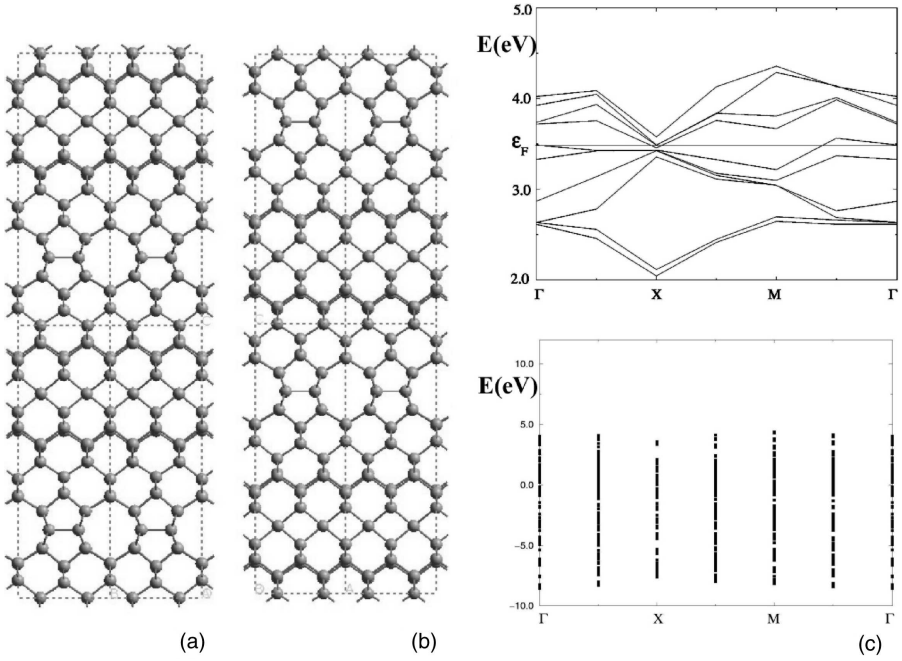

Fig. 4. The structural unit of the bonded Pmm(m) interface: (a) [1 1 0]-, (b) [1 $\bar{1}$ 0]-projection of the 2 × 2 supercell, and (c) DFT-LDA band structure (overview and enlarged gap region).

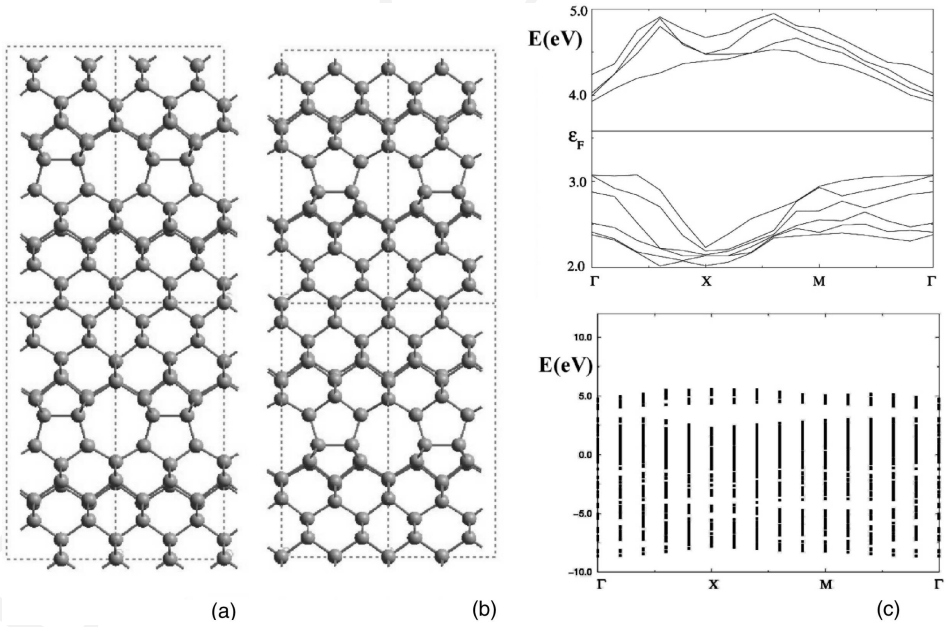

Fig. 5. The $\bar{4}2m$ -dreidl as structural unit of the bonded P($\bar{4}$)m2 interface: (a) [1 1 0]-, (b) [1 $\bar{1}$ 0]- projection of the 2 × 2 supercell, and (c) DFT-LDA band structure (overview and enlarged gap region).

indicating the insulating properties, the Pmmm interface behaves like a semi-metal. This may offer band gap tayloring by controlling the structure of bonded interfaces.

6. Hypothetical low density configurations

Finally, two hypothetical Si crystals are constructed by stacking the basic unit of the 90° twist boundary in several distinct ways. The two smallest structures, which can be built by a three dimensional arrangement of $\bar{4}2m$-dreidls, are shown in Figs. 6 and 7, together with their DFT-LDA band structures. The dreidl arrangements are of the type staggered and layered (cf. Figs. 6 and 7) having 12 and 24 atoms in the unit cell, respectively. Both structures are insulators with a large indirect band gap of approximately 0.9 and 1.4 eV. The hypothetical structures enable a new class of low-density silicon phases to be investigated by means of ab initio calculations. Thus these results may be related directly to the search of low-density materials as discussed in the following.

Under compression, silicon undergoes a phase transformation to the β-tin phase and, at higher pressures, to phases denoted as SiXI, SiV, SiVI and SiVII with Imma, simple hexagonal, Cmca or hcp structures, respectively (cf., e.g., Crain et al. [26] for a review). On pressure release and/or annealing, these phases transform to metastable bcc (BC8, SiIII) or rhobohedral (R8, SiXII) ones. All these structures and the phase transitions between them are subject to intensive studies because the local atomic arrangement is believed to be very similar to the amorphous phase and can therefore serve as theoretical model of amorphous silicon. Much less is known about phases of lower density compared to the density of the diamond cubic phase, mainly because of the difficulty of applying "*negative pressure*". In order to obtain more open structures one may incorporate a number of impurity atoms around which Si atoms can nucleate and remove the impurity atoms by further processing [24]. For silicon, clathrate structures can be formed by such a process [27], Ge structures with a low content of impurities have also been reported. A second, theoretical, route to search for new materials is to start from a complex compound structure and to predict new elemental materials. Demkov et al. [28] proposed a range of possible low-density silicon structures by stripping-off the

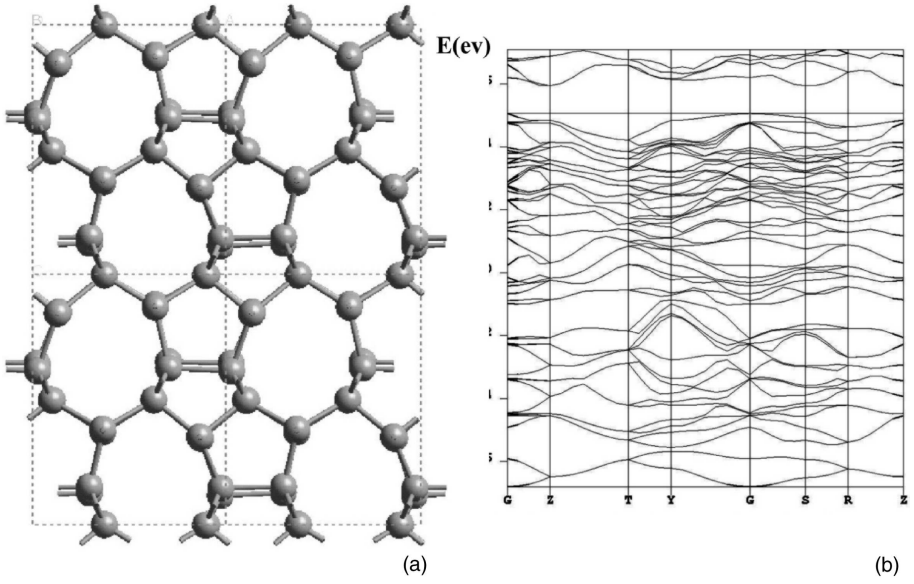

Fig. 6. DFT-LDA band structure (b) of a hypothetical "dreidl crystal" (a) with 12 atoms within the unit cell.

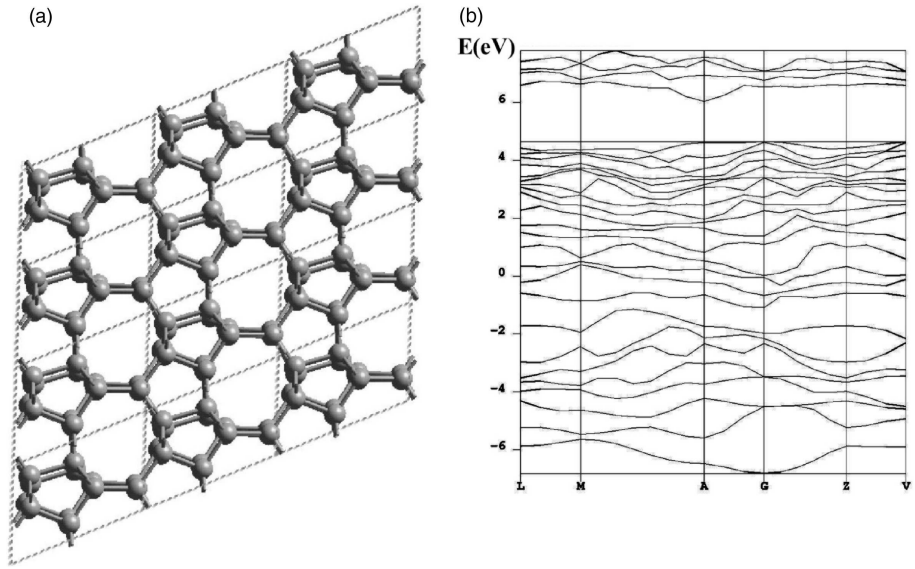

Fig. 7. DFT-LDA band structure (b) of a hypothetical "dreidl crystal" (a) with 24 atoms within the unit cell.

oxygen atoms of alumino-silicates and replacing aluminum by silicon. By such a procedure it is possible to generate systematically four-fold coordinated "*zeolites without oxygen*". All these structures are relatively low in energy. In particular, most of them are even lower in energy than the high-density phases β-tin and BC8. Another, also theoretical way to generate new structures is to define some basic structural unit and to repeat these unit in a certain manner to build a crystal. Chadi [29] proposed several low-density structures for Si and Ge by repeating a structural unit motivated by experimental studies on *allo*-Ge with a unit cell containing 128 atoms [30]. Perhaps suitable dreidl arrangements may offer an alternative structuring of low density phases.

7. Conclusion

MD simulations based on empirical potentials are used to investigate the elementary steps of bonding two Si(0 0 1) wafers. Calculated bonding energies and forces strongly depend on surface termination, oxides, adsorbates, and process control. Twisted starting configurations result in special interface configurations, which may be characterized by structural units, mostly no longer perfectly coordinated. For two of the configurations having low energies in the empirical MD simulations the band structures are estimated using DFT-LDA calculations. They reveal completely different electronic properties which may yield to a transition from insulator to semi-metal if the interface structure may be controlled by the bonding process. The space filling arrangement of dreidls enable to construct hypothetically low density Si material, which is an insulator, probably tunable by wafer bonding, too. However, the simulations lead to a better understanding of the physical processes at the interfaces and support the experimental investigations.

References

[1] Q.-Y. Tong, U. Gösele, Semiconductor Wafer Bonding: Science and Technology, Wiley, New York, 1999.
[2] A. Plößl, G. Kräuter, Mater. Sci. Eng. R 25 (1999) 1.
[3] C.M. Goringe, D.R. Bowler, E. Hernandez, Rep. Prog. Phys. 60 (1997) 1447.
[4] D. Conrad, K. Scheerschmidt, Phys. Rev. B 58 (1998) 4538.
[5] D.G. Pettifor, I.I. Oleinik, Phys. Rev. B 59 (1999) 8487.
[6] D. Conrad, K. Scheerschmidt, U. Gösele, Appl. Phys. A 62 (1996) 7.

[7] D. Conrad, K. Scheerschmidt, U. Gösele, Appl. Phys. Lett. 71 (1997) 2307.
[8] A.Y. Belov, D. Conrad, K. Scheerschmidt, U. Gösele, Philos. Mag. A 77 (1998) 55.
[9] A.Y. Belov, K. Scheerschmidt, U. Gösele, Phys. Status Solidi 171 (1999) 159.
[10] A.Y. Belov, R. Scholz, K. Scheerschmidt, Philos. Mag. Lett. 79 (1999) 531.
[11] C. Koitzsch, D. Conrad, K. Scheerschmidt, U. Gösele, J. Appl. Phys. 88 (2000) 7104.
[12] J. Tersoff, Phys. Rev. B 38 (1989) 9902.
[13] J. Tersoff, Phys. Rev. B 39 (1989) 5566.
[14] D. Conrad, K. Scheerschmidt, U. Gösele, Appl. Phys. Lett. 71 (2000) 49.
[15] K. Scheerschmidt, D. Conrad, A. Belov, H. Stenzel, Electrochem. Soc. Proc. 97-36 (1998) 381.
[16] M. Mostoller, M.F. Chisholm, T. Kaplan, Phys. Rev. Lett. 72 (1994) 1494.
[17] F.H. Stillinger, T.A. Weber, Phys. Rev. B 31 (1985) 5262.
[18] A.J. Dyson, P.V. Smith, Surf. Sci. 355 (1996) 140.
[19] S. Balamane, T. Halicioglu, W.A. Tiller, Phys. Rev. B 46 (1992) 2250.
[20] M.I. Baskes, Phys. Rev. B 46 (1992) 2727.
[21] M.C. Payne, M.P. Teter, D.C. Allen, T.A. Arias, J.D. Joanopolous, Rev. Mod. Phys. 64 (1992) 1045.
[22] D. Vanderbilt, Phys. Rev. B 32 (1990) 8412.
[23] H.J. Monkhorst, J.D. Pack, Phys. Rev. B 13 (1976) 5188.
[24] G.B. Adams, M. O'Keeffe, A.A. Demkov, O.F. Sankey, Y.M. Huang, Phys. Rev. B 49 (1994) 8048.
[25] K. Scheerschmidt, Mat. Res. Soc. Proc. 681E (2001) I2.3.
[26] J. Crain, G.J. Ackland, S.J. Clark, Rep. Prog. Phys. 58 (1995) 705.
[27] V.E. Dmitrienko, M. Kleman, F. Mauri, Phys. Rev. B 60 (1999) 9383.
[28] A.A. Demkov, W. Windl, O.F. Sankey, Phys. Rev. B 53 (1996) 11288.
[29] D.J. Chadi, Phys. Rev. B 32 (1985) 6485.
[30] A. Grüttner, R. Nesper, H.G. von Schnering, Angew. Chem. 94 (1982) 933.

UNCORRECTED PROOF